Dermatopontin Interacts with Fibronectin, Promotes Fibronectin Fibril Formation, and Enhances Cell Adhesion*[S]

Aiko Kato[‡], Osamu Okamoto[§1], Kazushi Ishikawa[§], Hideaki Sumiyoshi[¶], Noritaka Matsuo[¶], Hidekatsu Yoshioka[¶], Motoyoshi Nomizu[‖], Tatsuo Shimada[2], and Sakuhei Fujiwara[§]**

From the Departments of [‡]Plastic Surgery, [§]Dermatology, and [¶]Biochemistry and the [**]Faculty of Medicine, Oita University, 1-1 Idaigaoka, Hasama-machi, Yufu-shi, Oita 879-5593, Japan and the [‖]Laboratory of Clinical Biochemistry, School of Pharmacy, Tokyo University of Pharmacy and Life Sciences, 1432-1, Horinouchi, Hachioji, Tokyo 192-0392, Japan

We report that dermatopontin (DP), an abundant dermal extracellular matrix protein, is found in the fibrin clot and in the wound fluid, which comprise the provisional matrix at the initial stage of wound healing. DP was also found in the serum but at a lower concentration than that in wound fluid. DP co-localized with both fibrin and fibronectin on fibrin fibers and interacted with both proteins. Both normal fibroblast and HT1080 cell adhesion to the fibrin-fibronectin matrix were dose-dependently enhanced by DP, and the adhesion was mediated by $\alpha5\beta1$ integrin. The cytoskeleton was more organized in the cells that adhered to the fibrin-fibronectin-DP complex. When incubated with DP, fibronectin formed an insoluble complex of fibronectin fibrils as visualized by electron microscopy. The interacting sites of fibronectin with DP were the first, thirteenth, and fourteenth type III repeats (III_1, III_{13}, and III_{14}), with III_{13} and III_{14} assumed to be the major sites. The interaction between III_{2-3} and III_{12-14} was inhibited by DP, whereas the interaction between I_{1-5} and III_{12-14} was specifically and strongly enhanced by DP. Because the interaction between III_{2-3} and III_{12-14} is involved in forming a globular conformation of fibronectin, and that between I_{1-5} and III_{12-14} is required for forming fibronectin fibrils, DP promotes fibronectin fibril formation probably by changing the fibronectin conformation. These results suggest that DP has an accelerating role in fibroblast cell adhesion to the provisional matrix in the initial stage of wound healing.

Dermatopontin (DP)[3] is a 22-kDa protein located in the extracellular matrix (ECM), comprising about 12 mg/kg wet dermis (1, for a review, see Ref. 2). It was initially purified from bovine dermis together with decorin (3). To date, over 10 dermatopontin homologues have been identified in five different mammalian species (2, 4–7) and in 12 different invertebrates (2).

DP has multiple activities. It induces fibroblast cell adhesion probably via integrin-type receptors (8). DP accelerates collagen fibrillogenesis and modifies the newly formed collagen fibrils (9). DP-knock-out mice demonstrate an Ehlers-Danlos phenotype (10), showing an abnormal ECM architecture and tissue flexibility in response to mechanical forces. Previously, we have shown that DP interacts with decorin and with transforming growth factor-$\beta1$ (11). Thus, it is suggested that DP has an ability to interact with multiple proteins, thereby forming a functional supramolecular complex in the ECM. Recently, we showed that DP promotes strong epidermal cell adhesion via $\alpha3\beta1$ integrin and syndecan (12). Considering this together with the fibroblast adhesion findings, we hypothesize that DP plays multiple roles in wound healing.

Just after wounding, extravasated blood forms a provisional matrix, which is an ECM composed mainly of fibrin and fibronectin (Fn) and a liquid component known as the wound fluid. The Fn in the provisional matrix serves as an adhesion and migration scaffold for fibroblasts in the surrounding ECM and for circulation-derived cells (13, 14).

In tissues, Fn is activated and assembled into a fibrillar structure known as the Fn matrix, which is found during both embryonic development and wound healing (15, 16). The only authentic molecular species known to promote Fn fibril formation are integrins (17–19), among which $\alpha5\beta1$ integrin would be the most recognized (20). A recombinant peptide, called anastellin, is the only non-integrin molecule that can promote Fn fibril formation (21). The Fn fibrils produced by anastellin have properties similar to those formed by integrins, and the fibrils are termed superfibronectin (21).

During an investigation of the biological activities of DP *in vivo*, we found that DP was present in the provisional matrix. We further found that DP interacted with Fn and fibrin and that DP enhanced the cell adhesion activity of Fn. We then demonstrated that DP promoted Fn fibril formation. This report describes the possible biological functions of DP in dermal wound healing. We demonstrate that DP is the first non-integrin ECM molecule that can activate Fn and initiate the formation of Fn fibrils.

EXPERIMENTAL PROCEDURES

Materials—DP was purified from newborn calf dermis, and an anti-DP carboxyl-terminal peptide antibody was produced as reported previously (1). This antibody does not cross-react with fibronectin, fibrinogen, fibrin, or albumin. Human plasma
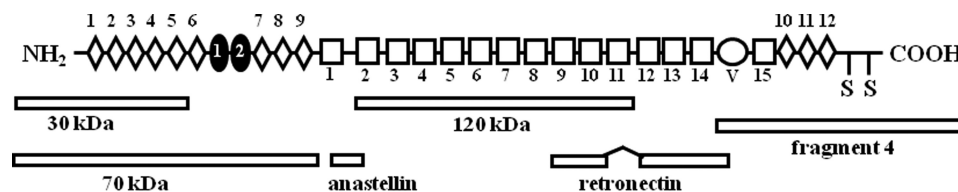
FIGURE 1. **Schematic representation of plasma Fn monomer structure and Fn fragments.** Type I, II, and III repeats are represented by *diamonds, filled ovals,* and *boxes*, respectively. A V region is denoted by a *circle*. Numbers of each repeat are shown *within* or *near* each repeat. Positions of commercially available Fn fragments are shown at the *bottom*.

Fn, an anti-Fn mouse monoclonal antibody, 30-kDa and 70-kDa thermolysin fragments, a recombinant fragment of the first type III repeat (III$_1$) of fibronectin known as anastellin, and a 120-kDa chymotryptic fragment of Fn were purchased from Sigma. Retronectin, which is a bacterially expressed fragment spanning between III$_9$ and an amino-terminal part of the V region of Fn lacking III$_{11}$, was purchased from TaKaRa Chemical (Tokyo, Japan). Fluorescein isothiocyanate (FITC)-conjugated phalloidin was purchased from Sigma-Aldrich. Gradient slab gel, Readygel J 5–15%, was purchased from Bio-Rad, and a protein A-conjugated affinity gel, Dynabeads protein A, was purchased from Invitrogen. A carboxyl-terminal fragment beginning with a V region of Fn, namely fragment 4, was purchased from R & D Systems (Minneapolis, MN). A monomer plasma Fn structure and positions of these fragments within Fn are shown in Fig. 1. Function-blocking anti-integrin subunit antibodies (FB12 for α1, P1E6 for α2, ASC-1 for α3, P1H4 for α4, P1D6 for α5, M9 for αv, NKI-GoH3 for α6, and 6S6 for β1) and human fibrinogen were from Chemicon (Temecula, CA). An ECL reagent, nickel-Sepharose CL-4B, thrombin, and anti-His$_6$ antibody were purchased from GE Healthcare. Anti-fibrinogen antibody and anti-α5 and β1 integrin subunit antibodies were purchased from Santa Cruz Biotechnology, Inc. (Santa Cruz, CA). Anti-vinculin antibody was purchased from Enzo Life Sciences International (Plymouth Meeting, PA). A rhodamine-labeled anti-rabbit IgG antibody, FITC-labeled anti-mouse and anti-goat IgG antibodies, and nonimmune mouse IgG were purchased from Jackson ImmunoResearch Laboratories, Inc. (West Grove, PA). Sulfo-NHS-LC-biotin, HRP-conjugated streptavidin, and BCA reagent were purchased from Pierce. Specimens from patients were taken with the patients' consent, according to the guidelines of the Ethical Council of Oita University.

Cell Culture—Normal human fibroblasts and cells of a human fibrosarcoma-derived fibroblast cell line, HT1080, were cultured as a monolayer in 75-cm^2 bottles at 37 °C in a humidified 5% CO$_2$, 95% air atmosphere. The cells were maintained in DMEM containing 10% (v/v) FCS.

Immunohistochemistry and Western Blotting—A fibrin clot taken from a 2-day-old burn bulla in the forearm of a 24-year-old female was embedded in Tissue-Tek® O.C.T. compound (Sakura Finetek, Torrance, CA). Four-μm sections were made, rinsed in PBS, blocked with 1% defatted skim milk in PBS, and incubated with either anti-DP and anti-Fn antibodies or anti-DP and anti-fibrinogen antibodies for 30 min, followed by incubation with a rhodamine-labeled anti-rabbit IgG antibody and an FITC-labeled anti-mouse IgG antibody, respectively, with three 10-min intervals of rinsing with PBS. The incubated

sections were observed using a fluorescent Optiphot-2 microscope (Nikon, Tokyo, Japan).

For detection of DP, crude samples of the serum and the wound fluid taken from the surgical wound of a patient were first fractionated using a gel filtration column, TSK gel G-3000 SWXL (7.5 × 300 mm) (Tosoh, Tokyo, Japan), in 50 mM Tris/HCl, 0.5 M NaCl, 6 M urea, pH 7.5. The flow was 0.5 ml/min, and 0.5-ml fractions were collected. The fractions were separated using a 12% T, 0.3% C Tricine SDS-PAGE (22) under reducing conditions and were Western blotted onto a PVDF membrane. DP was identified with an anti-DP rabbit antibody, followed by incubation with an HRP-conjugated anti-rabbit IgG antibody. For Fn detection, the crude samples were separated by 5% SDS-polyacrylamide gels under reducing conditions, and after Western blotting, Fn was probed with an anti-Fn mouse antibody and HRP-conjugated anti-mouse antibody. Bands were visualized using an ECL reagent.

Immunoprecipitation—The fibrin clot was extracted with 50 mM Tris/HCl, pH 7.5, containing 0.2, 0.5, and 1% deoxycholate successively at 4 °C. Anti-Fn mouse IgG and nonimmune mouse IgG were coated on gels of Dynabeads protein A, and the immunoprecipitation was performed according to the manufacturer's protocol, using PBS containing deoxycholate as a wash buffer. The gel was extracted with sample buffer for electrophoresis, and the samples were run on Tricine SDS-polyacrylamide gels under reducing condition and Western blotted. DP was visualized as described above.

Cell Adhesion Assay—Fibrinogen was coated on a 96-well plate (Assist, Tokyo, Japan) at 5 μg/ml in 0.14 M NaCl, 30 mM phosphate buffer, pH 7.3, overnight at room temperature. Then the wells were rinsed once with PBS, and thrombin in PBS was added at 1 unit/ml and was incubated for 1 h at room temperature. After rinsing with PBS, the wells were blocked by 1% BSA in PBS for 6 h, followed by a wash with PBS. Then Fn and/or DP in PBS was added to the wells and was incubated overnight at room temperature. Then the wells were rinsed with PBS three times. A monolayer of normal fibroblasts was detached with 5 mM EDTA in PBS, and the cells were suspended in DMEM. The cells were inoculated in the wells at 30,000 cells/100 μl/well and were incubated at 37 °C in an incubator. After incubation, the wells were rinsed once with warm PBS, and the attached cells were fixed with 1% glutaraldehyde for 30 min and then stained with 0.1% crystal violet for 1 h. After staining, the wells were rinsed with running water, dried, and photographed. Finally, the dye was eluted with 0.1% Triton X-100 for 30 min, and absorbance at 595 nm was measured with a UV spectrometer ELX808 (BioTek, Winooski, VT). Cell adhesion was measured at 1 h of incubation, and unless otherwise mentioned, the

TABLE 1
Primer sequences

Product	Amino acid position	Sense primer sequence	Antisense primer sequence
Fn III$_1$	609–700	5′–GAATTCGGTGGTGGTGAAGTCAAAGCG–3′	5′–GGATCCCAGACCTATCCAAGCTCAAGT–3′
Fn III$_{1-2}$	609–809	5′–GAATTCTGTTGTTTGTGAAGTAGACAG–3′	5′–GGATCCCAGACCTATCCAAGCTCAAGT–3′
Fn III$_2$	719–809	5′–GAATTCTGTTGTTTGTGAAGTAGACAG–3′	5′–GGATCCTCTCCTCTTGTGGCCACTTCT–3′
Fn III$_3$	810–905	5′–GAATTCATCTGAGCGTGGGGTGCCAGT–3′	5′–GGATCCGCGCCTGATGCCCCTCCTGAC–3′
Fn III$_{2-3}$	719–905	5′–GAATTCATCTGAGCGTGGGGTGCCAGT–3′	5′–GGATCCTCTCCTCTTGTGGCCACTTCT–3′
Fn III$_{12}$	1721–1812	5′–GAATTCCTCCAGAGTGGTGACAACTCC–3′	5′–GGATCCGCTATTCCTGCACCAACTGAC–3′
Fn III$_{13}$	1813–1901	5′–GAATTCAGTGGAGGCGTCGATGACCAC–3′	5′–GGATCCAATGTCAGCCCACCAAGAAGG–3′
Fn III$_{14}$	1902–1991	5′–GAATTCTGTCTTTTTCCTTCCAATCAG–3′	5′–GGATCCGCCATTGATGCACCATCCAAC–3′
Fn III$_{12-14}$	1721–1991	5′–GAATTCTGTCTTTTTCCTTCCAATCAG–3′	5′–GGATCCGCTATTCCTGCACCAACTGAC–3′
Fn V	1992–2102	5′–GAATTCACCGTGTGGGTACAGGTGATA–3′	5′–GGATCCGACGAGCTTCCCCAACTGGTA–3′
Fn III$_{15}$	2103–2182	5′–GAATTCCTTATGCCTCTGCTGGTCTTT–3′	5′–GGATCCCCGGGACTCAATCCAAATGCC–3′

volume of solution was 100 μl/well except for blocking by BSA and elution by Triton X-100, where 300 μl/well and 50 μl/well were used, respectively. For HT1080 cell adhesion, the fibrinogen concentration was 20 μg/ml.

Immunofluorescent Staining—All of the procedures were done at room temperature, except for the cell adhesion, which was performed at 37 °C. Spots (about 5 mm in diameter) on the surface of a siliconized glass plate (Dako Japan, Kyoto, Japan) were coated with 10 μl of fibrinogen at 20 μg/ml in PBS overnight. Then, after rinsing with PBS, the coated fibrinogen was converted to fibrin by incubating with 10 μl of thrombin at 1 unit/ml in PBS for 1 h and then blocked by 1% BSA in PBS for 6 h. Ten μl of Fn and DP mixture (20 μg/ml and 10 μg/ml, respectively) in PBS was applied to the spot of immobilized fibrin and was incubated overnight. In control experiments, DP was replaced by the same concentration of BSA and identically processed. Fibroblasts at a density of 30,000 cells/20 μl of DMEM were applied to the spot, and the cells were allowed to adhere for 1 h. After rinsing with PBS, the adhered cells were fixed with 3.7% formaldehyde in PBS for 5 min, rinsed in PBS, and then dehydrated in acetone for 5 min followed by rehydration in PBS. Permeabilization was performed in 0.1% Triton X-100 for 10 min, followed by rinsing in PBS. Actin filaments were stained with FITC-conjugated phalloidin in PBS. Vinculin was stained with anti-vinculin antibody followed by rhodamine-labeled anti-rabbit antibody. The buffer was PBS containing 10% nonfat dried milk. An α5 integrin subunit was stained with anti-α5 integrin antibody. The secondary antibody and the buffer were the same as described above. Finally, the samples were embedded in immersion oil. For HT1080 cell adhesion, the concentrations of Fn, DP, and BSA were 10 μg/ml, respectively.

Production of Recombinant Type III Repeats and V Region of Fn—All Fn domains were expressed using a pCOLD® bacterial expression system (TaKaRa Bio, Tokyo, Japan) using *Escherichia coli* BL-21 as a host. Using this system, recombinant proteins were expressed in principle as the amino-terminally His$_6$-tagged form. The His$_6$ tag is connected with enzyme cleavage sequences and with additional amino acids originating from multiple cloning sites. A reverse transcription product of cultured human fibroblasts was used as a template for PCR amplification of a DNA sequence encoding Fn domains. Antisense primers were designed to have a BamHI sequence, and sense primers were designed to have an EcoRI sequence at the 5′-ends, respectively. The DNA sequences and positions of primers within DNA/amino acid sequences of Fn are indicated in Table 1. PCR was performed using combinations of the primers, and the products were ligated into a TEasy vector (Promega, Madison, WI) and then were cloned into *E. coli* XL-1. The vectors carrying the correct inserts were digested with BamHI and EcoRI, and the fragments of the inserts were then ligated to corresponding sites of pCOLD I vectors and were transfected into *E. coli* BL-21. A construct of Fn V was made using a pCOLD-TF vector because the construct in the pCOLD-I vector did not express any fusion protein for unknown reasons.

Expression of fusion proteins of type III repeats and a V region of Fn was performed at 15 °C for 24 h according to the manufacturer's instructions using a pCOLD bacterial expression system. The bacteria were collected by centrifugation. The pellet was digested with 1 mg/ml lysozyme in 50 mM Tris/HCl, pH 8.0, containing 0.14 M NaCl (TBS) for 1 h on ice and then was extracted by adding Nonidet P-40 at a final concentration of 0.2% and sonicated. After the extract was cleared by centrifugation, the supernatant was applied to a nickel-Sepharose CL 4B column; washed with 20 mM sodium phosphate buffer, 0.5 M NaCl, and 40 mM imidazole, pH 7.4 (starting buffer); and eluted with 20 mM sodium phosphate buffer, 0.5 M NaCl, and 0.5 M imidazole (elution buffer), pH 7.4, according to the manufacturer's instructions. The expression of recombinant proteins was determined by Western blotting probed with an anti-His$_6$ antibody. The recombinant proteins were extensively dialyzed against PBS. The concentration of the proteins was determined by a BCA reagent, and BSA was used as a standard.

A Fn V region expressed using a pCOLD-TF vector appears as a fusion protein with His$_6$-tagged transcription factor (TF). The fusion protein was adsorbed to a nickel-Sepharose CL-4B column as described above, and the gel was rinsed with PBS. Thrombin was added to the gel in PBS and incubated for 2 h at room temperature. After digestion, the gel was rinsed with PBS. Thrombin was present in an unbound fraction, and the liberated recombinant Fn V from the TF was associated with the gel. The recombinant Fn V was eluted from the gel with a starting buffer containing 1 M NaCl and was processed as described above. SDS-PAGE patterns of these recombinant Fn fragments are shown in the supplemental Fig. 1.

Biotinylation of Fragments—A 30-kDa thermolysin fragment of Fn and recombinant Fn type III repeats were labeled with sulfo-NHS-LC-biotin according to the manufacturer's instructions. Briefly, the fragments in PBS were incubated with a 20-fold excess molar concentration of sulfo-NHS-LC-biotin in PBS for 2 h at room temperature. The reaction was terminated
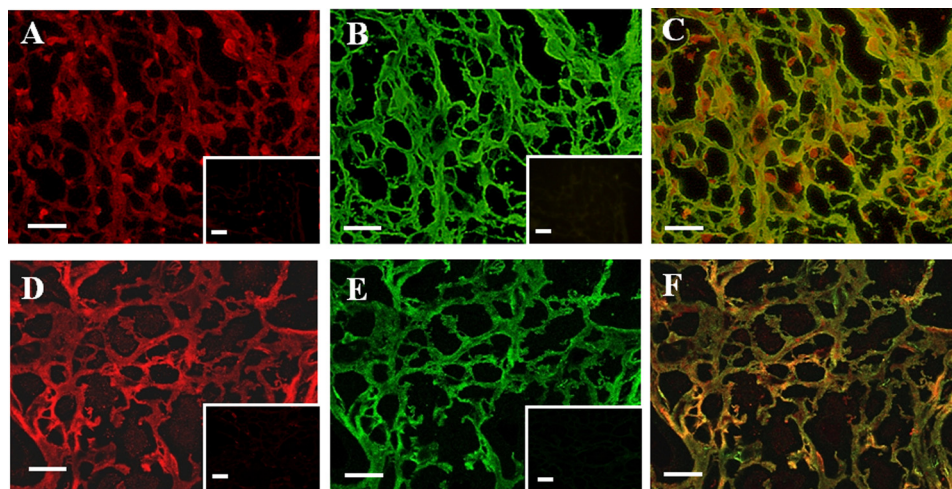
FIGURE 2. **Immunofluorescent images of Fn and DP in a fibrin clot.** A fibrin clot was double stained with an anti-DP rabbit antibody (*A*) and anti-Fn mouse antibody (*B*), an anti-DP rabbit antibody (*D*), and an anti-fibrinogen mouse antibody (*E*). These antibodies were detected by a rhodamine-labeled anti-rabbit antibody and an FITC-labeled anti-mouse antibody, respectively. In the *insets* in *A*, *B*, *D*, and *E*, the primary antibodies were replaced with either preimmune serum or IgG, followed by incubation with the secondary antibodies. *C* and *F*, *merged images* of *A* and *B* and of *D* and *E*, respectively. *Bars*, 20 μm.

by incubation with triethanolamine in Tris/HCl, pH 7.5, at a final concentration of 10 mM for 1 h at room temperature. The labeled proteins were dialyzed against PBS, and labeling was confirmed by Western blotting probed by HRP-conjugated streptavidin. The labeled protein concentrations were determined as described above.

Solid-phase Assay for Protein Interaction—All procedures were carried out at room temperature. Fn and the recombinant domains in 30 mM sodium phosphate buffer, 0.14 M NaCl, pH 7.3 (PB-Na), were immobilized on a 96-well plate overnight. For fibrin immobilization, fibrin was formed as described above. The wells were then rinsed with PBS and were blocked with 1% BSA in PBS for 6 h. After rinsing with PBS, either DP, Fn, labeled recombinant Fn domains, or the mixture dissolved in PB-Na containing 0.05% Tween 20 (PB-Na-Tw) was added into the wells and was incubated overnight. In the following procedure, incubation was done in PB-Na-Tw for 2 h, and rinsing was done with the same buffer. DP was probed with an anti-DP antibody, followed by HRP-conjugated anti-rabbit IgG antibody. Fn was probed with an anti-Fn monoclonal antibody followed by a HRP-conjugated anti-mouse IgG antibody. Biotinylated Fn domains were probed by HRP-conjugated streptavidin. Color was allowed to develop by adding 0.057 M citric acid, 0.086 M disodium hydrogen phosphate containing 10 mM 2,2′-azido-bis (3-ethylbenzothiazoline-6-sulfonic acid) and 0.03% hydrogen peroxide in the dark. The color reaction was terminated by adding aliquots of 0.1 M citric acid containing 1.5 mM sodium azide, after which absorbance at 405 nm was determined.

Fibril-forming Assay—Fn fibril formation was assessed according to a previous report (23). Briefly, 0.5 μM Fn in 50 mM Tris/HCl, pH 8.0, containing 0.14 M NaCl, was centrifuged, and any insoluble material was removed. Then DP at 30 μM in the same buffer was added to the Fn solution and incubated for 16 h at room temperature. The reaction volume was 10 μl. After incubation, the mixture was centrifuged, and the pellets were rinsed once with the Tris buffer. Pellets and supernates were applied to 5–15% gradient gels (Bio-Rad) under reducing con-

ditions and were stained by Coomassie Brilliant Blue R-250. For control, BSA at 30 μM was mixed with Fn and was identically processed.

Electron Microscopy—One μM fibronectin was incubated with 8 μM DP in PBS at room temperature for 8 h. The samples were placed on a poly-L-lysine-coated coverglass and were immobilized at room temperature for 10 h in a wet chamber. The samples were then treated with Karnovsky solution, washed with cacodylic acid, stained with 1% OsO_4 and 1% tannic acid, dehydrated, dried, and coated with OsO_4. All of the observations and photographs were performed with a scanning electron microscope (S-4800, Hitachi, Japan) operated at an acceleration voltage of 15 kV.

RESULTS

DP Is Present in the Provisional Matrix and in the Wound Fluid—Double immunofluorescent staining of DP and Fn in a fibrin clot revealed that DP was present in a net-like structure of fibrin (Fig. 2*A*). Fn was also stained in a similar pattern (Fig. 2*B*) as demonstrated in a merged image (Fig. 2*C*). The staining of DP overlapped with Fn in the periphery of the fibrillar structure. Thus, DP partially overlaps with Fn. DP was also stained in a similar partial overlap pattern with fibrin, which was probed by anti-fibrinogen antibody (Fig. 1, *D–F*).

The fibrin clot was extracted with TBS containing deoxycholate. Fn and DP were extracted by TBS containing 1% deoxycholate, but the yield was low (data not shown). Immunoprecipitation by anti-Fn antibody and anti-fibrinogen antibodies probed with anti-DP antibody did not demonstrate a positive DP band (data not shown). Therefore, whether DP interacts with Fn or fibrin could not be confirmed by this approach.

Wound fluid, which is a soluble fraction of the provisional matrix, was electrophoresed on a Tricine SDS-polyacrylamide gel and Western blotted. DP as well as Fn were present in the wound fluid (Fig. 3, *lanes 2* and *5*). Interestingly, DP was also found in the serum (*lanes 3*). Although the staining intensity of Fn was similar between the wound fluid and the serum (*lanes 5*
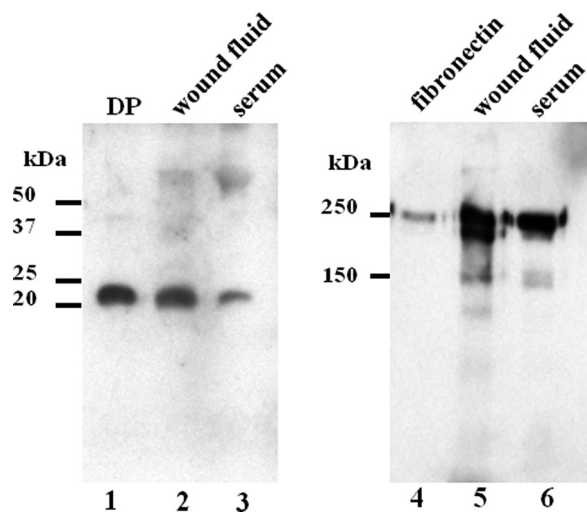
FIGURE 3. **Western blotting of the wound fluid and the serum.** *Lanes 1–3*, detection of DP. *Lane 1*, a DP standard. *Lanes 2* and *3*, DP in the wound fluid and in the serum, respectively. *Lanes 4–6*, detection of Fn. *Lane 4*, a Fn standard. *Lanes 5* and *6*, Fn in the wound fluid and in the serum, respectively. Molecular mass values are indicated at the *left* of *lanes 1* and *4*.

and *6*), the relative intensity of DP in the wound fluid was much greater than that in the serum (Fig. 3, *lanes 2* and *3*), suggesting that the DP concentration is elevated in the wound.

DP Interacts with Fn and Fibrin and enhances the interaction— DP showed a dose-dependent interaction with immobilized Fn, and immobilized DP also interacted with Fn (Fig. 4, *A* and *B*). DP interacted with immobilized fibrin in a manner similar to that of Fn (Fig. 4*C*), whereas immobilized DP did not show evident interaction with fibrin in a liquid phase (data not shown). DP demonstrated much weaker interaction with immobilized fibrinogen (data not shown), suggesting that a higher order structure of fibrin is required for an interaction with DP, as is the case for the Fn-fibrinogen/fibrin interaction (24, 25).

Next, the interaction between Fn and fibrin was examined in the presence of DP. Fn interacted with fibrin as reported previously (data not shown) (24). The interaction between fibrin and Fn was strongly enhanced by DP in a dose-dependent manner (Fig. 4*D*). From these results, DP is hypothesized to form a ternary complex with Fn and fibrin.

DP Enhances Fibroblast Adhesion to the Fn-Fibrin Complex— We examined if the DP-Fn-fibrin ternary complex enhances cell adhesion. When increasing concentrations of DP form a complex with Fn and fibrin, fibroblast adhesion to the complex was greatly enhanced in a dose-dependent manner (Fig. 5*A*). In comparison, BSA did not induce this enhancement, and the level of adhesion remained near background level. When background cell adhesion was subtracted, the enhancement of cell adhesion by DP was about 10-fold.

Next, a panel of antibodies was examined for inhibition of cell adhesion. Fibroblast adhesion to the ternary complex of fibrin-Fn-DP was significantly inhibited by anti-$\alpha 5$ and -$\beta 1$ integrin subunit antibodies (Fig. 5*B*). Thus, $\alpha 5\beta 1$ integrin was the cell surface receptor involved in fibroblast cell adhesion to the fibrin-Fn-DP complex.

Many of the adhered fibroblasts to the fibrin-Fn-DP complex were well spread (Fig. 6*A*), whereas most of those that adhered
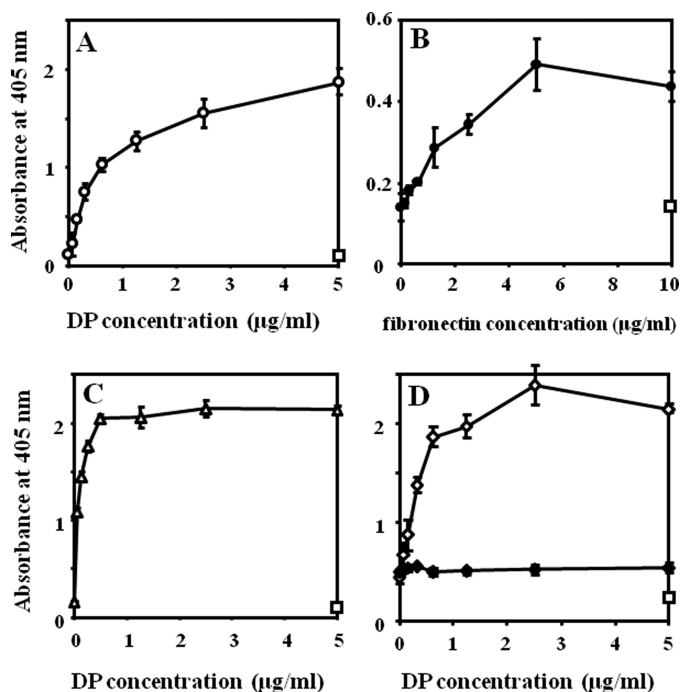

FIGURE 4. **Interaction profiles of DP with Fn and/or fibrin.** *A*, interaction of DP with Fn. Fn was immobilized in wells at 5 μg/ml, DP was added at the concentrations indicated on the *x* axis, and bound DP was detected as described under "Experimental Procedures." *B*, interaction of Fn with DP. DP was immobilized at 5 μg/ml, and Fn was added and detected. *C*, fibrin was immobilized at 5 μg/ml, and DP was added and detected. In *A–C*, *rectangles* indicate nonspecific interaction of DP or Fn at the indicated concentrations with the plate where ligand immobilization was omitted. *D*, enhancement of interaction between Fn and fibrin by DP. Fibrin was immobilized at 10 μg/ml, and a mixture of Fn at 5 μg/ml and DP at the indicated concentrations was applied to the fibrin ($\diamond$). Fn and BSA were mixed and applied to the fibrin ($\blacklozenge$). Bound Fn was detected as described. A *rectangle* indicates the nonspecific reaction in a condition where Fn was omitted from the fibrin-Fn-DP interaction and probed by anti-Fn antibody. A representative absorbance of the highest DP concentration is shown. In *A–D*, experiments were performed three times in triplicate, and means ± S.D. are shown.

to the fibrin-Fn complex were not (Fig. 6*B*). The fibroblasts that adhered to the ternary complex developed an organized linear actin cytoskeleton and vinculin in a dot-like pattern (Fig. 6, *C* and *E*), whereas those that adhered to the fibrin-Fn complex showed a poor organization of actin cytoskeleton and vinculin (Fig. 6, *D* and *F*). The integrin $\alpha 5$ and $\beta 1$ staining showed a fine granular pattern, and the staining appeared slightly enhanced in the cells that adhered to the ternary complex (Fig. 6, *G–J*).

Another cell line, HT1080, demonstrated an almost identical profile of cell adhesion enhancement by DP (supplemental Fig. 2). The cytoskeleton and integrin profiles were similar to those in the case of fibroblasts, although the organization of the actin cytoskeleton was less developed than that of fibroblasts (supplemental Fig. 3).

Upon gross examination, fibroblast adhesion patterns to the ternary complex of fibrin-Fn-DP and to the binary complex of fibrin-Fn were not greatly different (*photographs* in Fig. 5*A*). Interestingly, HT1080 cells demonstrated different patterns of cell adhesion to the ternary and the binary complexes. When DP is present, HT1080 cells adhered to the ternary complex in a homogenous, sheetlike pattern (*photographs* in supplemental Fig. 2*A*), whereas in the absence of DP, the pattern of the cells that adhered to the Fn-fibrin complex was much less organized.
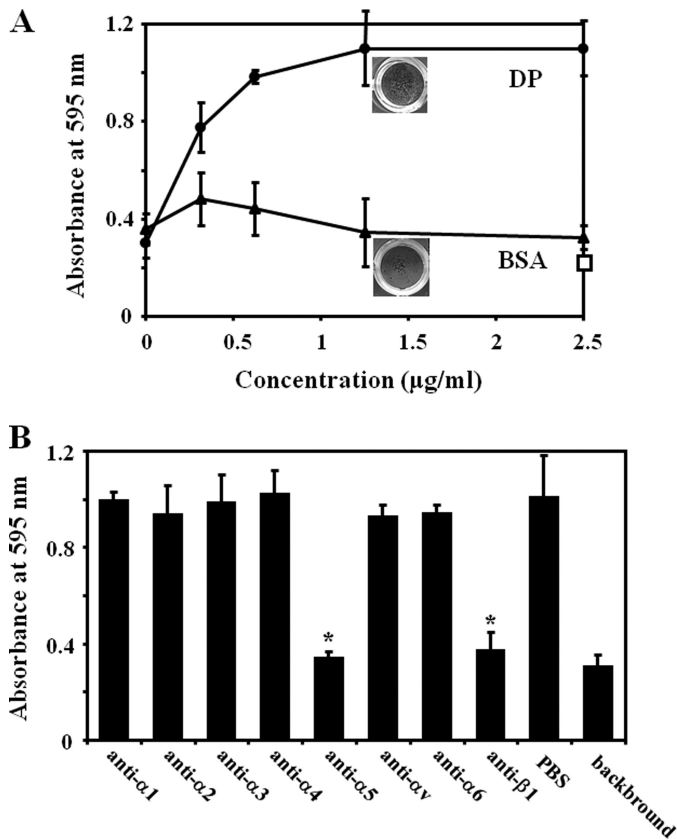
FIGURE 5. *A*, enhancement of cell adhesion to the fibrin-Fn-DP ternary complex. Fibrin was immobilized, and then mixtures of Fn at 1 μg/ml and DP (●) at the concentrations indicated on the *x* axis were applied to the wells. Normal fibroblasts were incubated, and cell adhesion was quantified as described under "Experimental Procedures." For a control, DP was replaced with BSA (▲) and identically processed. A *rectangle* indicates the cell adhesion to fibrin-DP complex at the indicated concentration. Experiments were performed three times in triplicate, and means ± S.D. are shown. The appearance of the cells is shown in the *panel*. *Photographs* were taken after adhered cells were stained and dried. The *top panel* indicates a well in which a ternary complex was formed at DP concentration of 1.25 μg/ml. The *bottom panel* represents a well in which a Fn-fibrin-BSA complex at the same concentration is formed. *B*, inhibition of cell adhesion to the fibrin-Fn-DP complex by anti-integrin function-blocking antibodies. Antibodies were mixed with fibroblasts in suspension, and the cells were allowed to adhere. PBS was added to the cell suspension as a control. Antibody concentrations were 10 μg/ml. *, $p < 0.01$. Data are expressed as mean ± S.D. of triplicate results. Experiments were performed three times and gave similar results.

From these results, we concluded that DP not only enhances the amount of Fn that interacts with fibrin but also induces a structural change in Fn.

DP Induces Formation of Superfibronectin—The enhancement of the cell adhesion to Fn by DP is consistent with the formation of fibronectin fibrils. Therefore, we tested for Fn fibril formation. When Fn is activated and forms fibrils, it becomes insoluble (23). We next determined whether an insoluble pellet of Fn was formed in the presence of DP. As shown in Fig. 7*A*, in the presence of DP, most of the Fn forms an insoluble large pellet that migrates above the Fn monomer, indicating the formation of Fn fibrils. The larger band as well as the Fn monomer reacted with the anti-Fn antibody; therefore, the larger band was proved to be a polymer of Fn (Fig. 7*A*, *lanes 7* and *8*). The major portion of DP remained in the supernatant fraction, as shown by a band around 22 kDa (Fig. 7*A*, *lane 3*), and a minor fraction of DP is associated with the pellet fraction (*lane 4*). In
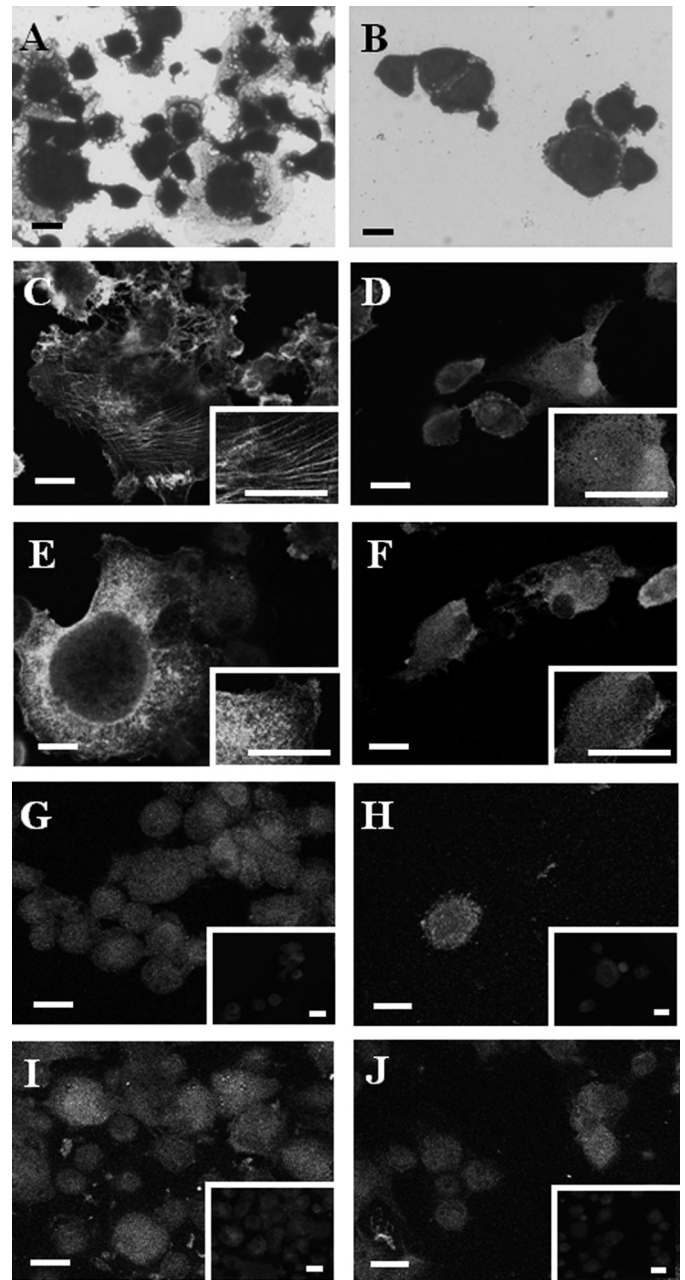
FIGURE 6. **Morphologies of the adhered fibroblasts and cytoskeletal organization.** *A* and *B*, crystal violet staining of the fibroblasts. Appearance of the cells from Fig. 5*A*. *A*, cells that adhered to a ternary complex of fibrin-Fn-DP; *B*, cells that adhered to a complex of fibrin-Fn-BSA. *C*, *E*, *G*, and *I*, fluorescence staining of cells that adhered to the fibrin-Fn-DP complex. *D*, *F*, *H*, and *J*, corresponding staining of cells that adhered to the fibrin-Fn-BSA complex. *C* and *D*, phalloidin staining. *E* and *F*, vinculin staining. The *insets* in *C–F* represent a higher magnification of the staining. Negative controls of vinculin staining demonstrated a background staining (data not shown). *G* and *H*, integrin α5 subunit staining. *I* and *J*, integrin β1 subunit staining. In *E–J*, the *inset* in each *panel* represents a negative control as described under "Experimental Procedures." *Bars*, 20 μm.

contrast, incubation of Fn by itself or with BSA formed a faint larger molecular mass pellet, but the amount was much less than that formed in the presence of DP (*lanes 2* and *6*).

To confirm the formation of Fn fibrils, the insoluble pellet was examined by scanning electron microscopy. As expected, Fn formed numerous fibrils when incubated with DP (Fig. 7*B*, *1*). The fibrils were 50–200 nm in diameter, irregular, and tor-
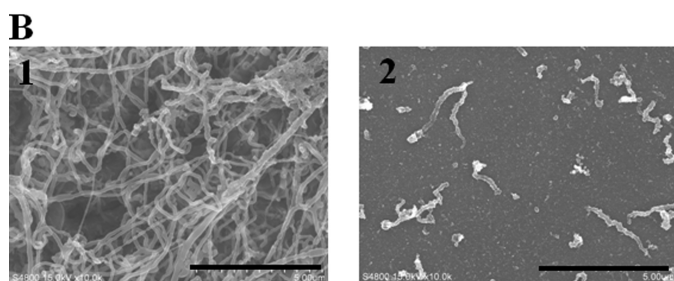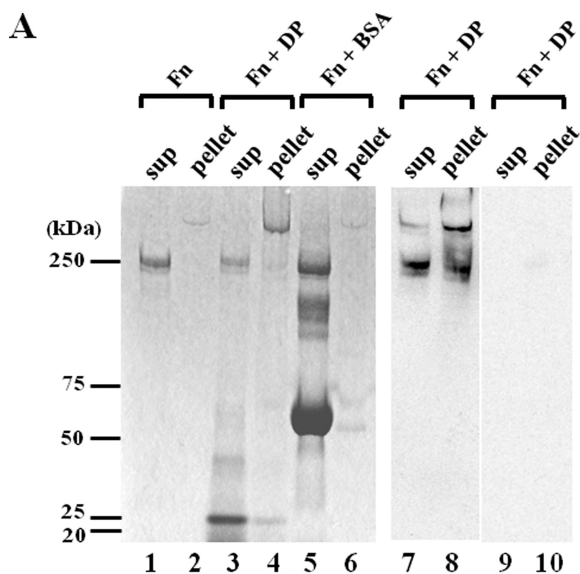
FIGURE 7. **Fn fibril formation by DP.** *A*, *lanes 1* and *2*, the supernatant and the pellet of Fn alone. *Lanes 3* and *4*, supernatant and pellet of a mixture of Fn with DP. *Lanes 5* and *6*, supernatant and pellet of a mixture of Fn with BSA. *Lanes 7* and *8*, bands in *lanes 3* and *4* were Western blotted and probed with anti-Fn antibody. *Lanes 9* and *10*, negative controls of *lanes 7* and *8* probed by nonimmune mouse IgG. Molecular masses are indicated on the *left*. *B*, scanning electron microscopy of the Fn fibrils. *1*, Fn incubated with DP; *2*, Fn incubated without DP. *Bars*, 5 μm.
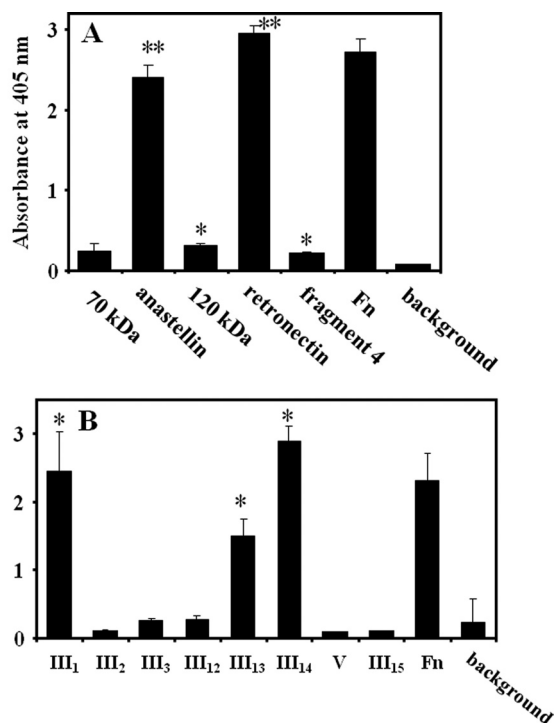

FIGURE 8. **Determination of the binding sites of Fn with DP.** *A*, screening of Fn fragments that interact with DP. Fn and Fn fragments indicated on the *x* axis were immobilized in wells at 2 μg/ml. DP was added to the wells at 2 μg/ml, and the interaction was monitored as described under "Experimental Procedures." *background*, absorbance of 2 μg/ml DP added to noncoated wells. *, $p < 0.01$ compared with a value of background absorbance. **, $p < 0.01$ compared with that of a 120-kDa fragment. *B*, determination of Fn domains that interact with DP. Recombinant Fn domains were immobilized in wells at 10 μg/ml. Fn was immobilized at 2 μg/ml. The following procedures are the same as those described above. In *A* and *B*, experiments were performed three times in triplicate, and means ± S.D. (*error bars*) are shown. *background*, absorbance of noncoated wells incubated with the same concentration of DP. *, $p < 0.01$ compared with a value of background absorbance.

tuous. These features were similar to those of the fibronectin fibrils formed on the cell surface as reported previously (26). In contrast, in the absence of DP, Fn formed some short aggregates, but it never formed the long fibrillar structures seen in the presence of DP (Fig. 7*B*, *2*). The small aggregates may reflect the faint Fn band in the pellet fraction on SDS-PAGE in Fig. 7*A* (*lane 2*). DP alone did not form fibrils except for sparse tiny aggregates (data not shown). These results suggest that DP induces Fn fibril formation.

Major Interaction Sites of Fn with DP are III_{13} and III_{14}—We investigated the binding sites on Fn for DP, using Fn fragments (Fig. 1). Two fragments, anastellin and retronectin, strongly interacted with DP (Fig. 8*A*). Other fragments demonstrated statistically significant but relatively weak interactions (Fig. 7*A*). DP interacted more strongly with retronectin than with an overlapping 120-kDa fragment, indicating that the binding sites locate within a stretch between III_{12} and V. To further identify the binding sites, type III repeats around the candidate region were expressed in *E. coli*, and their binding to DP was examined. As shown in Fig. 8*B*, DP demonstrated strong interaction with III_1, III_{13}, and III_{14}, but it did not bind to other domains.

Because complex domains of III_{1-2} as well as III_{12-14} are known to be important for Fn fibril formation (27–29), we also

expressed these domains in tandem fashion and examined the interaction with DP. DP failed to interact with III_{1-2}, but it interacted with III_{12-14} at a similar level as it did with III_{14} (data not shown). Functional and structural analyses of III_{1-2} reveal that this domain has a specific structure and is primarily cryptic (30, 31); nevertheless, the domain is involved in Fn fibril formation. Considering this together with the fact that DP failed to interact with III_{1-2}, we conclude that III_1 is a potential or a cryptic DP interaction site and that the main DP interaction sites are III_{13} and III_{14}.

DP Modifies Interdomain Interactions of Fn—For Fn fibril formation, interactions between I_{1-5} and other domains (within which are III_{1-2} and III_{12-14}) are necessary (27–29). Interestingly, these type III repeats were also DP binding sites, as shown in Fig. 8*B*. Therefore, the influence of DP on the interaction of the 30-kDa fragment (I_{1-5}) with these domains was examined. DP did not enhance the interaction between I_{1-5} and III_{1-2}, whereas an interaction between I_{1-5} and III_{12-14} was greatly enhanced by the presence of DP (Fig. 9*A*). As a control, an interaction between I_{1-5} and III_{15} was relatively unaffected by DP. Another important interaction between III_{2-3} and III_{12-14}, which is crucial for maintaining a compact conformation of native Fn (32), was partially disrupted by DP (Fig. 9*B*).
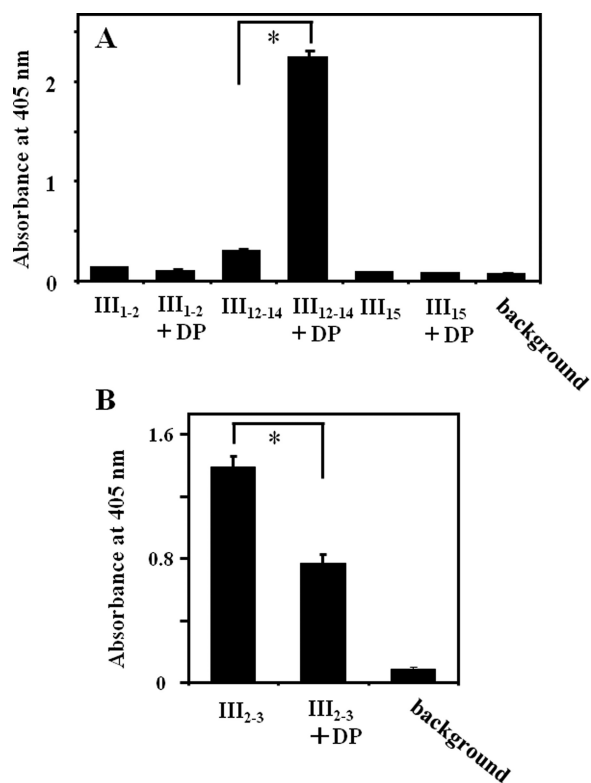
FIGURE 9. **Modification of interdomain interactions of Fn by DP.** *A*, enhancement of the interaction by DP. Recombinant Fn domains shown on the *x* axis were immobilized in wells at 20 μg/ml. A biotinylated 30-kDa fragment of Fn was added at 5 μg/ml in the presence or absence of 10 μg/ml DP. *B*, inhibition of the interaction by DP. Recombinant III_{12-14} was immobilized at 1 μg/ml, and biotinylated III_{2-3} was added at 0.2 μg/ml in the presence or absence of 2 μg/ml DP. The bound 30-kDa fragment and the III_{2-3} were probed by a streptavidin-conjugated HRP as described under "Experimental Procedures." *, $p < 0.01$. Experiments were performed three times in triplicate, and means $\pm$ S.D. (*error bars*) are shown.

These data show that DP would change Fn conformation by modifying inter- and intramolecular interactions.

DISCUSSION

In this study, we found that DP is present in the provisional wound matrix, the wound fluid, and in the serum in addition to the ECM. The presence of DP in the serum was unexpected, and the function of DP in the serum is not known. It is possible that DP functions as a coagulation factor because an 18-kDa invertebrate homologue of DP from blood cells of a crab shell, *Limulus polyphemus*, is an agglutination factor (33). DP in the provisional matrix may derive from either the serum or the interstitial fluid. The presence of DP in the provisional matrix and in the wound fluid is a novel finding, and this is the first observation that DP may play a role in wounds.

DP-kockout mice exhibit an Ehlers-Danlos syndrome phenotype (10). The previous report focused on the change of the ECM architecture. Because patients with Ehlers-Danlos syndrome demonstrate delayed wound healing and abnormal scar formation (34, 35), the knock-out mice would be expected to have a similar phenotype, but this has not been examined. From a functional aspect, DP not only makes a ternary complex with Fn and fibrin but also enhances the interaction. On the other hand, immobilized DP showed less and no interaction with liq-

uid phase Fn and fibrin, respectively. These findings indicate a possibility that the binding site of DP is partially or completely cryptic in the solid phase. The enhancement of the Fn interaction with fibrin in the presence of DP contributes to an increase in cell adhesion as shown in Fig. 5. The cells that adhered to the ternary complex demonstrated increased spreading and a more organized cytoskeleton, indicating that the cells undergo morphological changes beyond adhesion on the complex.

Koblinski *et al.* (36) reported that co-immobilization of Fn with nonadhesive proteins, such as BSA and cytochrome *c*, on an artificial surface induced a strong cell adhesion enhancement. This study importantly elucidated that Fn conformation can be changed when it is simultaneously immobilized with several nonadhesive proteins, even with BSA. In the present study, fibrin was immobilized first, and then complexes were formed on the fibrin. In our system, a mixture of Fn and BSA did not enhance cell adhesion, whereas a mixture with DP did. Therefore, we confirmed that the observed cell adhesion enhancement was specifically induced by DP, and the mechanism of the enhancement was different from that in the previous report (36).

In this study, we found that DP promoted Fn fibril formation. An interaction between III_{2-3} and III_{12-14} is reported to be necessary for maintaining the compact and inactive conformation of Fn (32). Once activated by integrins, multiple interdomain interactions are created between conformationally transformed Fn molecules, and Fn fibrils are formed (37). For Fn fibril formation, the presence of I_{1-5} is essential (37, 38), and interactions between I_{1-5} and III_{1-2} (27, 28) and/or I_{1-5} and III_{12-14} (29) are reported to play very important roles.

The major interaction sites of Fn with DP were determined to be III_{13} and III_{14}, and a potential or cryptic site was III_1. All of these domains are involved in a formation of Fn fibrils. The finding that an interaction between I_{1-5} and III_{12-14} was enhanced strongly and that between III_{2-3} and III_{12-14} was considerably inhibited by DP supports the idea that the change of the interaction between these domains of Fn and DP promotes Fn fibril formation. Because the interaction between I_{1-5} and III_{1-2} was not enhanced by DP, it is likely that the III_{1-2} is cryptic as previously reported (30, 31). However, it is possible that these domains unfold as other interdomain interactions are disrupted as described below (23).

Apart from integrins, anastellin is the only known non-integrin type protein that can induce superfibronectin formation (21). The binding site of Fn to anastellin is III_3, and a conformational change of cryptic III_{1-2} follows the interaction (23). The binding site on Fn for anastellin locates within an interaction site between III_{2-3} and III_{12-14}, as in the case for DP, indicating that domain unfolding of a Fn molecule is important for Fn fibril formation.

Anastellin is an artificial III_1 domain of Fn that lacks A and B β-sheets covering one-third of the amino terminus of the domain (21, 39). On the other hand, DP is an endogenous protein that is found in many types of tissues, with the dermis being the most abundant source. Therefore, it is possible that DP plays a role as a natural activator of Fn in a provisional matrix before fibroblasts or endothelial cells migrate and interact with Fn via $\alpha 5\beta 1$ integrin.

Although DP is an abundant protein within the ECM, its biological functions remain largely unknown. In this report, DP was shown to be present in the provisional wound matrix, and, more importantly, DP was found to be the first non-integrin protein that can activate Fn and induce Fn fibril formation. Thus, in a context of Fn activation, DP may help a wound to heal by accumulating in the wound either from the surrounding ECM or from the serum.

REFERENCES

1. Okamoto, O., Suzuki, Y., Kimura, S., and Shinkai, H. (1996) *J. Biochem.* **119,** 106–114
2. Okamoto, O., and Fujiwara, S. (2006) *Connect. Tissue Res.* **47,** 177–189
3. Neame, P. J., Choi, H. U., and Rosenberg, L. C. (1989) *J. Biol. Chem.* **264,** 5474–5479
4. Cronshaw, A. D., MacBeath, J. R., Shackleton, D. R., Collins, J. F., Fothergill-Gilmore, L. A., and Hulmes, D. J. (1993) *Matrix* **13,** 255–266
5. Superti-Furga, A., Rocchi, M., Schäfer, B. W., and Gitzelmann, R. (1993) *Genomics* **17,** 463–467
6. Tzen, C. Y., and Huang, Y. W. (2004) *Exp. Cell Res.* **294,** 30–38
7. Takemoto, S., Murakami, T., Kusachi, S., Iwabu, A., Hirohata, S., Nakamura, K., Sezaki, S., Havashi, J., Suezawa, C., Ninomiya, Y., and Tsuji, T. (2002) *Basic Res. Cardiol.* **97,** 461–468
8. Lewandowska, K., Choi, H. U., Rosenberg, L. C., Sasse, J., Neame, P. J., and Culp, L. A. (1991) *J. Cell Sci.* **99,** 657–668
9. MacBeath, J. R., Shackleton, D. R., and Hulmes, D. J. (1993) *J. Biol. Chem.* **268,** 19826–19832
10. Takeda, U., Utani, A., Wu, J., Adachi, E., Koseki, H., Taniguchi, M., Matsumoto, T., Ohashi, T., Sato, M., and Shinkai, H. (2002) *J. Invest. Dermatol.* **119,** 678–683
11. Okamoto, O., Fujiwara, S., Abe, M., and Sato, Y. (1999) *Biochem. J.* **337,** 537–541
12. Okamoto, O., Hozumi, K., Katagiri, F., Takahashi, N., Sumiyoshi, H., Matsuo, N., Yoshioka, H., Nomizu, M., and Fujiwara, S. (2010) *Biochemistry* **49,** 147–155
13. Midwood, K. S., Mao, Y., Hsia, H. C., Valenick, L. V., and Schwarzbauer, J. E. (2006) *J. Invest. Dermatol. Symp. Proc.* **11,** 73–78
14. Diegelmann, R. F., and Evans, M. C. (2004) *Front. Biosci.* **9,** 283–289
15. Hynes, R. O. (1990) *Fibronectins*, Springer-Verlag, New York
16. Muro, A. F., Chauhan, A. K., Gajovic, S., Iaconcig, A., Porro, F., Stanta, G., and Baralle, F. E. (2003) *J. Cell Biol.* **162,** 149–160
17. Wennerberg, K., Lohikangas, L., Gullberg, D., Pfaff, M., Johansson, S., and Fässler, R. (1996) *J. Cell Biol.* **132,** 227–238
18. Wu, C., Hughes, P. E., Ginsberg, M. H., and McDonald, J. A. (1996) *Cell Adhes. Commun.* **4,** 149–158
19. Sechler, J. L., Cumiskey, A. M., Gazzola, D. M., and Schwarzbauer, J. E. (2000) *J. Cell Sci.* **113,** 1491–1498
20. Fogerty, F. J., Akiyama, S. K., Yamada, K. M., and Mosher, D. F. (1990) *J. Cell Biol.* **111,** 699–708
21. Morla, A., Zhang, Z., and Ruoslahti, E. (1994) *Nature* **367,** 193–196
22. Schägger, H., and von Jagow, G. (1987) *Anal. Biochem.* **166,** 368–379
23. Ohashi, T., and Erickson, H. P. (2005) *J. Biol. Chem.* **280,** 39143–39151
24. Makogonenko, E., Tsurupa, G., Ingham, K., and Medved, L. (2002) *Biochemistry* **41,** 7907–7913
25. Makogonenko, E., Ingham, K. C., and Medved, L. (2007) *Biochemistry* **46,** 5418–5426
26. Peters, D. M., Portz, L. M., Fullenwider, J., and Mosher, D. F. (1990) *J. Cell Biol.* **111,** 249–256
27. Aguirre, K. M., McCormick, R. J., and Schwarzbauer, J. E. (1994) *J. Biol. Chem.* **269,** 27863–27868
28. Hocking, D. C., Sottile, J., and McKeown-Longo, P. J. (1994) *J. Biol. Chem.* **269,** 19183–19187
29. Bultmann, H., Santas, A. J., and Peters, D. M. (1998) *J. Biol. Chem.* **273,** 2601–2609
30. Ingham, K. C., Brew, S. A., Huff, S., and Litvinovich, S. V. (1997) *J. Biol. Chem.* **272,** 1718–1724
31. Vakonakis, I., Staunton, D., Rooney, L. M., and Campbell, I. D. (2007) *EMBO J.* **26,** 2575–2583
32. Johnson, K. J., Sage, H., Briscoe, G., and Erickson, H. P. (1999) *J. Biol. Chem.* **274,** 15473–15479
33. Fujii, N., Minetti, C. A., Nakhasi, H. L., Chen, S. W., Barbehenn, E., Nunes, P. H., and Nguyen, N. Y. (1992) *J. Biol. Chem.* **267,** 22452–22459
34. Viglio, S., Zoppi, N., Sangalli, A., Gallanti, A., Barlati, S., Mottes, M., Colombi, M., and Valli, M. (2008) *J. Invest. Dermatol.* **128,** 1915–1919
35. Steinmann, B., Royce P. M., and Superti-Furga, A. (2002) in *Connective Tissue and Its Inherited Disorders*, pp. 431–523, Wiley-Liss, New York
36. Koblinski, J. E., Wu, M., Demeler, B., Jacob, K., and Kleinman, H. K. (2005) *J. Cell Sci.* **118,** 2965–2974
37. Mao, Y., and Schwarzbauer, J. E. (2005) *Matrix Biol.* **24,** 389–399
38. Schwarzbauer, J. E. (1991) *J. Cell Biol.* **113,** 1463–1473
39. Dickinson, C. D., Veerapandian, B., Dai, X. P., Hamlin, R. C., Xuong, N. H., Ruoslahti, E., and Ely, K. R. (1994) *J. Mol. Biol.* **236,** 1079–1092